Excitonic pairing of two-dimensional Dirac fermions near the antiferromagnetic quantum critical point

Hai-Xiao Xiao,[1] Jing-Rong Wang,[2] Zheng-Wei Wu,[1] and Guo-Zhu Liu[1,*]

[1]*Department of Modern Physics, University of Science and Technology of China, Hefei, Anhui 230026, People's Republic of China*

[2]*Anhui Province Key Laboratory of Condensed Matter Physics at Extreme Conditions, High Magnetic Field Laboratory of the Chinese Academy of Science, Hefei, Anhui 230031, People's Republic of China*

(Received 25 March 2019; published 17 June 2019)

Two-dimensional Dirac fermions are subjected to two types of interactions, namely, the long-range Coulomb interaction and the short-range on-site interaction. The former induces excitonic pairing if its strength α is larger than some critical value α_c, whereas the latter drives an antiferromagnetic Mott transition when its strength U exceeds a threshold U_c. Here, we study the impacts of the interplay of these two interactions on excitonic pairing with the Dyson-Schwinger equation approach. We find that the critical value α_c is increased by weak short-range interaction. As U increases to approach U_c, the quantum fluctuation of the antiferromagnetic order parameter becomes important and interacts with the Dirac fermions via the Yukawa coupling. After treating the Coulomb interaction and Yukawa coupling interaction on an equal footing, we show that α_c is substantially increased as $U \to U_c$. Thus, the excitonic pairing is strongly suppressed near the antiferromagnetic quantum critical point. We obtain a global phase diagram on the U-α plane and illustrate that the excitonic insulating and antiferromagnetic phases are separated by an intermediate semimetal phase. These results provide a possible explanation of the discrepancy between recent theoretical progress on excitonic gap generation and existing experiments in suspended graphene.

DOI: 10.1103/PhysRevB.99.245130

I. INTRODUCTION

Two-dimensional (2D) massless Dirac fermions are the low-energy excitations of a number of condensed matter systems. Examples include d-wave high-T_c cuprate superconductors [1,2], graphene [3–7], the surface of three-dimensional (3D) topological insulators [8], and organic conductor α-(BEDT-TTF)$_2$I$_3$ [9]. While the single-particle properties of Dirac fermion systems have already been extensively studied, the strong correlation effects are still not well understood. Ordinary metals are known to be robust against repulsive interactions [10], which renders the validity of Fermi liquid theory. In contrast, the repulsive interactions are much more important in two-dimensional (2D) Dirac fermion systems and may lead to several possible phase-transition instabilities [5–7,11]. Generically, there are two types of repulsive interactions, namely, long-range Coulomb interaction and Hubbard-like on-site interaction. The former is spin blinded, whereas the latter acts on two electrons with different spins and is thus spin distinguished.

When the strength parameter U of on-site repulsive interaction is greater than a critical value U_c, there is a quantum phase transition from gapless semimetal (SM) to antiferromagnetic (AFM) Mott insulator [12]. The SM-AFM quantum critical point (QCP) falls in the university class of the Gross-Neveu-Yukawa model [12]. Apart from the SM-AFM transition, Sato *et al.* [13] studied the transition between the SM and Kekulé valence-bond solid caused by on-site interaction. When other sorts of repulsions are considered, SM materials could exhibit richer phase-transition structures [13–20]. For instance, Raghu *et al.* [14] investigated the cooperative effects of nearest- and next-nearest-neighbor repulsions, and found a number of insulating phases, including charge density wave (CDW), AFM, and topological Mott phases that display quantum anomalous Hall (QAH) and quantum spin Hall (QSH) effects, although subsequent studies revealed that the topological Mott phases can be destroyed by fluctuations [17].

In case the Fermi level is located exactly at the band-touching point, the long-range Coulomb interaction is poorly screened due to the vanishing of density of states (DOS). If the Coulomb interaction is weak, the system remains gapless but the fermion velocity is substantially renormalized [7,21]. When the Coulomb interaction strength parameter α exceeds a critical value α_c, a finite energy gap is dynamically generated via the formation of excitonic-type particle-hole pairs [22–46]. This then turns the originally gapless SM into a gapped excitonic insulator (EI). Another interesting possibility is that the Coulomb-like interaction can induce an electron-electron pairing, as predicted and discussed in Refs. [47,48].

In previous works, the Coulomb interaction and the on-site interaction were usually investigated separately. Their interplay can give rise to intriguing properties, especially in the strong interaction regimes. Interesting progress has recently been made towards more detailed knowledge of this interplay. Tang *et al.* [18] have studied the influences of long-range Coulomb and on-site interactions on the ground-state properties of 2D Dirac fermion systems by combining the nonperturbative quantum Monte Carlo (QMC) simulation

*gzliu@ustc.edu.cn

and the renormalization group (RG) technique. Their work [18] reproduced the previously discovered logarithmic velocity renormalization and confirmed that the SM-AFM transition occurs at some critical value U_c. They further found that U_c increases as α grows, which indicates that the Coulomb interaction disfavors AFM transition. These results are summarized in the phase diagram shown in Fig. 1 of Ref. [18].

The results reported in Ref. [18] are only applicable to the region of weak Coulomb interaction. The region of strong Coulomb interaction appears to be inaccessible to the numerical methods developed in Refs. [18] and [19]. As aforementioned, strong Coulomb interaction is able to induce excitonic pairing and SM-EI transition. This problem has attracted broad interest in the past two decades. Extensive theoretical efforts have been devoted to examining whether the SM-EI transition can be realized in graphene. In Refs. [18,19], the influence of on-site interaction on the SM-EI transition has not been addressed. Moreover, it remains unclear how the SM-EI transition is affected by the SM-AFM quantum criticality.

In this paper, we study the excitonic pairing of 2D Dirac fermions by considering both the long-range Coulomb and on-site interactions. In particular, we will investigate the impact of on-site interaction on the fate of excitonic pairing. For small values of U, the Coulomb interaction and on-site interaction need to be treated on an equal footing. When U grows, the AFM correlation is gradually enhanced. As $U \to U_c$, the system approaches the AFM QCP and the quantum fluctuations of the AFM order parameter interact strongly with the Dirac fermions via the Yukawa-type coupling. To examine the influence of AFM quantum criticality on excitonic pairing, we need to study the interplay between the Coulomb interaction and the Yukawa coupling interaction.

The nonperturbative Dyson-Schwinger (DS) equation approach will be employed to compute the excitonic gap and to determine α_c. In our calculations, the series expansion is controlled by the small parameter $1/N$, where N is the spin degeneracy of a Dirac fermion. Within this framework, the Coulomb interaction parameter α can take any value. This allows us to access the strong Coulomb interaction regime. The Yukawa coupling can also be handled by the $1/N$ expansion. However, the on-site interaction is spin distinguished, to be explained below, and the $1/N$ expansion becomes invalid. In the case of weak on-site interaction, we will perform a weak-coupling expansion.

After incorporating the impact of weak on-site interaction, we find that the critical value α_c for EI transition is slightly increased. At the AFM QCP (U_c), the value of α_c is increased dramatically by the Yukawa coupling interaction. Indeed, α_c is an increasing function of Yukawa coupling constant λ. Apparently, excitonic pairing is significantly suppressed by the quantum fluctuation of the AFM order parameter. As U decreases from U_c, the system departs from AFM QCP and the suppression of excitonic pairing caused by AFM fluctuation is weakened. Combining these results with those reported in Ref. [18], we obtain a schematic global phase diagram on the U-α plane, shown in Fig. 1. It seems that the EI phase cannot be directly converted into an AFM Mott insulating phase: they are separated by an intermediate SM phase.

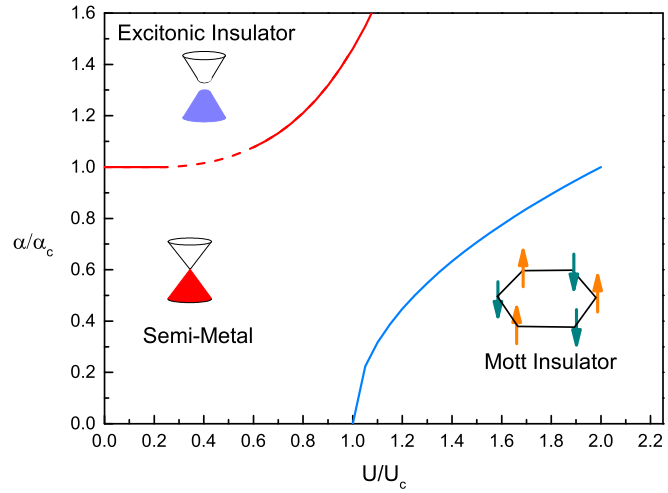

FIG. 1. The global phase diagram of a 2D Dirac fermion system on the plane spanned by Coulomb interaction parameter α and the on-site interaction parameter U. The critical line of U_c is taken from Ref. [18]. The solid part of the EI critical line is plotted based on our DS equation results, and the dashed part of this line is plotted based on extrapolation.

Our theoretical results provide a possible explanation of the discrepancy between recent theoretical progress and existing experiments in graphene. It is known that α takes its maximal value $\alpha = 2.16$ when graphene is suspended in vacuum. The zero-temperature ground state of suspended graphene should be an insulator if $\alpha_c < 2.16$. In a recent work, Carrington *et al.* [33] has performed a careful DS equation study by going beyond many of the previously used approximations and found that $\alpha_c \approx 2.0$, which is slightly below $\alpha = 2.16$. This result suggests that suspended graphene would be insulating at zero temperature. However, this is apparently at odds with previous experiments [21,49]. According to the analysis of Ref. [50], graphene seems to be close to the AFM QCP, and thus the impact of AFM quantum criticality on α_c needs to be seriously taken into account. Our results show that the proximity to AFM QCP substantially increases the critical value α_c, which makes the SM-EI transition very unlikely in realistic graphene.

The rest of the paper is organized as follows. In Sec. II, we present the DS equation for a dynamical excitonic gap. The gap equation is solved and analyzed in Sec. III, and the physical application of the result is discussed in Sec. IV. The results are summarized in Sec. V.

II. DYSON-SCHWINGER GAP EQUATION

The free 2D Dirac fermions are described by the Lagrangian in Minkowski space,

$$\mathcal{L}_0 = \sum_{\sigma} \bar{\Psi}_\sigma(\tau, \mathbf{x}) i(\gamma_0 \partial_0 - v\gamma_i \partial_i) \Psi_\sigma(\tau, \mathbf{x}), \qquad (1)$$

where Ψ_σ is a four-component spinor field and $\bar{\Psi}_\sigma = \Psi_\sigma^\dagger \gamma_0$. The index σ sums from 1 to N, with $N = 2$ being the spin degeneracy of the Dirac fermion. The 4×4 γ matrices are defined via Pauli matrices as $\gamma_{0,i} = \tau_3 \otimes (\sigma_3, i\sigma_2, -i\sigma_1)$, which

satisfy the Clifford algebra. The fermion velocity v is taken to be a constant.

We will consider three different sorts of interactions, including the long-range Coulomb interaction, the spinful on-site interaction, as well as the Yukawa coupling between Dirac fermions and AFM quantum fluctuation. If the system is far from the AFM QCP, we need to study only the first two interactions. But when the system is sufficiently close to the AFM QCP, the interplay of Coulomb interaction and Yukawa coupling should be carefully investigated. Below we present the effective field theories for these three interactions in order.

A. Pure Coulomb interaction

The pure Coulomb interaction can be modeled by the following Lagrangian:

$$\mathcal{L}_C = -ea_0 \sum_\sigma \bar{\Psi}_\sigma \gamma_0 \Psi_\sigma + a_0 \frac{|\nabla|}{2e^2} a_0, \tag{2}$$

where a_0 is an auxiliary scalar field introduced to represent Coulomb interaction. It is easy to verify that the Lagrangian $\mathcal{L}_0 + \mathcal{L}_C$ respects the continuous chiral symmetry $\Psi_\sigma \to e^{i\gamma_5\theta}\Psi_\sigma$, where $\gamma_5 = -\sigma_2 \otimes \sigma_0$ anticommutes with $\gamma_{0,i}$.

The pure long-range Coulomb interaction has already been widely studied [22–46]. In Refs. [11,48], Downing and Portnoi have considered the problem of electrostatic confinement of Dirac fermions and found a zero-energy bielectron bound state in scalar potentials. In this paper, we study only the excitonic particle-hole pairing realized in systems with a large number of Dirac fermions.

As mentioned in Sec. I, the Coulomb interaction can be studied within the framework of $1/N$ expansion. Below, we will adopt an approximation that retains only the leading-order contribution of $1/N$ expansion. To this order, the contribution of wave-function renormalization can be ignored. The free propagator of Dirac fermions is

$$G^0_\sigma(\omega, \mathbf{k}) = \frac{1}{\omega\gamma_0 - v(\gamma_1 k_x + \gamma_2 k_y)}. \tag{3}$$

Interaction turns this free propagator into

$$G_\sigma(\omega, \mathbf{k}) = \frac{1}{\omega\gamma_0 - v(\gamma_1 k_x + \gamma_2 k_y) - m_\sigma(\omega, \mathbf{k})}, \tag{4}$$

where $m_\sigma(\omega, \mathbf{k})$ is the fermion mass function. Once $m_\sigma(\omega, \mathbf{k})$ acquires a finite value due to the Coulomb interaction, an excitonic mass gap is generated and the gapless SM is converted into a fully gapped EI. In order to examine whether an excitonic gap is generated, we write down the following DS equation:

$$m_\sigma(\varepsilon, \mathbf{p}) = \frac{1}{4}\int \frac{d\omega}{2\pi}\frac{d^2\mathbf{k}}{(2\pi)^2} \mathrm{Tr}[\gamma_0 G_\sigma(\omega, \mathbf{k})\gamma_0 V(\Omega, \mathbf{q})], \tag{5}$$

where $\Omega = \varepsilon - \omega$ and $\mathbf{q} = \mathbf{p} - \mathbf{k}$. Here, the effective Coulomb interaction is given by

$$V(\Omega, \mathbf{q}) = \frac{1}{V_0^{-1}(\Omega, \mathbf{q}) + \Pi_c(\Omega, \mathbf{q})}, \tag{6}$$

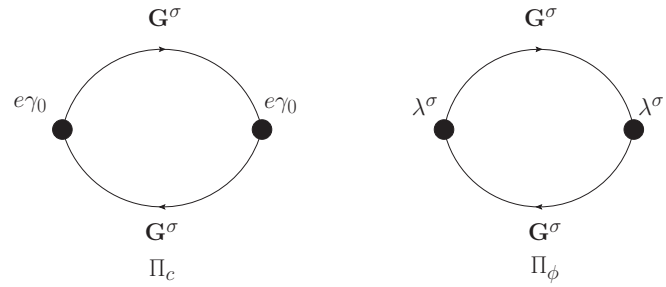

FIG. 2. Feynman diagrams of Π_c and Π_ϕ. The difference between two diagrams lies in the expression of the vertices.

where $\Pi_c(\Omega, \mathbf{q})$ is the polarization function and

$$V_0(\mathbf{q}) = \frac{2\pi e^2 \delta(t)}{\kappa|\mathbf{q}|} \tag{7}$$

is the bare Coulomb interaction, with $\kappa = \epsilon_0\epsilon_r$ being the dielectric constant. To the leading order of $1/N$ expansion, the Feynman diagram for $\Pi_c(\Omega, \mathbf{q})$ is shown in Fig. 2. At the random phase approximation (RPA) level, the one-loop Π_c is calculated as follows [22]:

$$\begin{aligned}\Pi_c(\Omega, \mathbf{q}) &= -N\int \frac{d\omega}{2\pi}\frac{d^2\mathbf{k}}{(2\pi)^2}\mathrm{Tr}\,[\gamma_0 G_0(\omega, \mathbf{k}) \\ &\quad \times \gamma_0 G_0(\omega + \Omega, \mathbf{k} + \mathbf{q})] \\ &= \frac{N}{8}\frac{\mathbf{q}^2}{\sqrt{v\mathbf{q}^2 - \Omega^2}}.\end{aligned} \tag{8}$$

After performing the Wick rotation ($\omega \to i\omega$), we get the following DS gap equation in Euclidean space [22]:

$$\begin{aligned}m_\sigma(\varepsilon, \mathbf{p}) &= \int \frac{d\omega}{2\pi}\frac{d^2\mathbf{k}}{(2\pi)^2}\frac{m_\sigma(\omega, \mathbf{k})}{\omega^2 + p_x^2 + p_y^2 + m_\sigma(\omega, \mathbf{k})^2} \\ &\quad \times \frac{1}{\frac{|\mathbf{q}|}{2\pi v\alpha} + \frac{N}{8}\frac{\mathbf{q}^2}{\sqrt{\Omega^2 + v^2\mathbf{q}^2}}},\end{aligned} \tag{9}$$

where a new parameter $\alpha = e^2/v\kappa$ is defined to measure the effective interaction strength. For a given flavor N, the above gap equation has a nontrivial solution, i.e., $m \neq 0$, only when $\alpha > \alpha_c$. The QCP between SM and EI phases is located at $\alpha = \alpha_c$. If the value of α is fixed, a nonzero gap could be generated only when $N < N_c$.

B. Weak on-site interaction

As shown by Herbut and collaborators [12,54], the generic on-site interaction is complex and can be decomposed into eight independent four-fermion coupling terms. Here, following Ref. [18], we consider only the spin-distinguished interaction term

$$\mathcal{L}_I = g\sum_\sigma (\sigma\bar{\Psi}_\sigma\Psi_\sigma)^2, \tag{10}$$

which is responsible for the transition into the AFM Mott insulating phase. In Ref. [18], this is referred to as the spinful Gross-Neveu (GN) interaction. It is also called the chiral Heisenberg GN interaction [51]. According to Ref. [12], g is

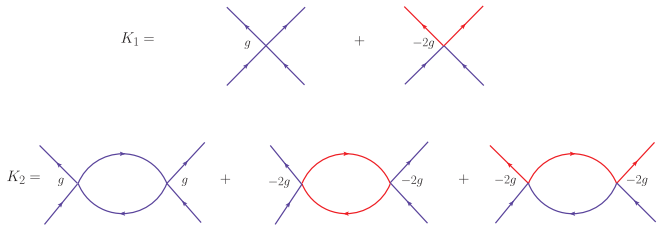

FIG. 3. Diagrams of leading (K_1) and subleading (K_2) order contributions to the GN interaction kernel. Blue and red solid lines stand for fermions with spin σ and spin $-\sigma$, respectively.

related to U through the identity $g = -\frac{Ua^2}{8}$, where a is the lattice spacing.

Upon expanding the quadratic term appearing in $\mathcal{L}_I$, we get two sorts of four-fermion couplings:

$$\mathcal{L}_I = g\sum_{\sigma} \bar{\Psi}_\sigma \Psi_\sigma \bar{\Psi}_\sigma \Psi_\sigma - 2g\bar{\Psi}_{\sigma_1}\Psi_{\sigma_1}\bar{\Psi}_{\sigma_2}\Psi_{\sigma_2}. \tag{11}$$

For a given spin σ, the coupling $\bar{\Psi}_\sigma \Psi_\sigma \bar{\Psi}_\sigma \Psi_\sigma$ amounts to the GN interaction with flavor $N = 1$. Such a coupling term cannot be treated by means of $1/N$ expansion. The coupling constant g has the dimension of inverse mass. It is convenient to define a dimensionless parameter $\tilde{g} = g\Lambda/v$, where the momentum cutoff Λ is connected to a via the relation $\Lambda \sim a^{-1}$. In the following, we will choose to carry out series expansion in powers of $\tilde{g}$. This method is invalid in the strong-coupling regime. Tang *et al.* [18] have numerically investigated the strong-coupling regime by means of QMC simulation and found that the system enters into an AFM Mott insulating phase once $|\tilde{g}|$ becomes sufficiently large.

We first ignore the Coulomb interaction and examine whether or not the pure spinful GN interaction leads to dynamical generation of the excitonic gap. According to the analysis of Ref. [52], the DS equation can be formally written as

$$G_\sigma^{-1} = \left(G_\sigma^0\right)^{-1} - \sum_{\sigma'} \mathrm{Tr}[K_{\sigma,\sigma'}G_\sigma] + \frac{1}{2}\sum_{\sigma'} \mathrm{Tr}\left[G_{\sigma'}\frac{\delta K_{\sigma,\sigma'}}{\delta G_\sigma}G_{\sigma'}\right], \tag{12}$$

where $K_{\sigma,\sigma'}$ is the four-fermion interaction kernel. $K_{\sigma,\sigma'}$ can be obtained from the sum of all the two-particle irreducible vacuum diagrams in the full fermion propagators [52], represented by $V_{2\mathrm{IR}}(G)$. $V_{2\mathrm{IR}}(G)$ is connected to the kernel $K_{\sigma\sigma'}$ in the following way:

$$V_{2\mathrm{IR}}(G) = \sum_{\sigma,\sigma'} \frac{1}{2}\mathrm{Tr}[G_\sigma K_{\sigma,\sigma'}G_{\sigma'}]. \tag{13}$$

In this paper, we will retain both the leading-order and sub-leading-order corrections. The corresponding Feynman diagrams are presented in Fig. 3.

The leading-order contributions to K are

$$(K_1)_{\sigma_1,\sigma_1} = \frac{v\tilde{g}}{\Lambda}, \quad (K_1)_{\sigma_1,\sigma_2} = -2\frac{v\tilde{g}}{\Lambda}. \tag{14}$$

The sub-leading-order contributions are

$$\begin{aligned}(K_2)_{\sigma_1,\sigma_1}(q) &= -\int \frac{d^3k}{(2\pi)^3}\mathrm{Tr}\left[\left(\frac{v\tilde{g}}{\Lambda}\right)^2 G^0_{\sigma_1}(k)G^0_{\sigma_1}(q+k)\right] \\ &\quad -\int \frac{d^3k}{(2\pi)^3}\mathrm{Tr}\left[\left(2\frac{v\tilde{g}}{\Lambda}\right)^2 G^0_{\sigma_2}(k)G^0_{\sigma_2}(q+k)\right] \\ &= -5\left(\frac{v\tilde{g}}{\Lambda}\right)^2 \Pi_g(q), \end{aligned} \tag{15}$$

$$\begin{aligned}(K_2)_{\sigma_1,\sigma_2}(q) &= -\int \frac{d^3k}{(2\pi)^3}\mathrm{Tr}\left[\left(2\frac{v\tilde{g}}{\Lambda}\right)^2 G^0_{\sigma_1}(k)G^0_{\sigma_2}(q+k)\right] \\ &= -4\left(\frac{v\tilde{g}}{\Lambda}\right)^2 \Pi_g(q), \end{aligned} \tag{16}$$

where $q \equiv (\Omega, \mathbf{q})$ and $k \equiv (\omega, \mathbf{k})$, and we define

$$\Pi_g(q) = \int \frac{d\omega}{2\pi}\frac{d^2\mathbf{k}}{(2\pi)^2}(2\pi)^3\mathrm{Tr}\left[G^0_{\sigma_i}(k)G^0_{\sigma_i}(q+k)\right], \tag{17}$$

which is independent of spin directions. After doing simple calculations, we find that $\Pi_g(q) = \frac{1}{4v^2}\sqrt{v^2\mathbf{q}^2 - \Omega^2}$. From Fig. 3, we see that the first two orders of corrections satisfy the relation [52] $\frac{\delta K_i}{\delta G} = 0$ for both $i = 1$ and $i = 2$. Therefore, the DS equation for fermion self-energy takes the form

$$\begin{aligned} i\Sigma_\sigma(\varepsilon, \mathbf{p}) &= -\sum_{\sigma'}\int \frac{d\omega}{2\pi}\frac{d^2\mathbf{k}}{(2\pi)^2}\mathrm{Tr}[i(K_1)_{\sigma,\sigma'}(\Omega,\mathbf{q})iG_{\sigma'}(\omega,\mathbf{k})] \\ &\quad + \sum_{\sigma'}\int \frac{d\omega}{2\pi}\frac{d^2\mathbf{k}}{(2\pi)^2}[i(K_2)_{\sigma,\sigma'}(\Omega,\mathbf{q})][iG_{\sigma'}(\omega,\mathbf{k})] \\ &= -\frac{v\tilde{g}}{\Lambda}\int \frac{d\omega}{2\pi}\frac{d^2\mathbf{k}}{(2\pi)^2}\mathrm{Tr}[G_\sigma(\omega,\mathbf{k})] + 9\left(\frac{v\tilde{g}}{\Lambda}\right)^2 \\ &\quad \times \int \frac{d\omega}{2\pi}\frac{d^2\mathbf{k}}{(2\pi)^2}(2\pi)^3\Pi_g(\Omega,\mathbf{q})G_\sigma(\omega,\mathbf{k}). \end{aligned} \tag{18}$$

In the small $\tilde{g}$ region, we ignore the fermion damping and velocity renormalization; thus the fermion self-energy can be identified as the excitonic mass gap. We derive the following DS gap equation:

$$\begin{aligned} m_\sigma(\varepsilon,\mathbf{p}) &= i\frac{4v\tilde{g}}{\Lambda}\int \frac{d\omega}{2\pi}\frac{d^2\mathbf{k}}{(2\pi)^2}\frac{m_\sigma(\omega,\mathbf{k})}{\omega^2 - v^2\mathbf{k}^2 - m_\sigma^2(\omega,\mathbf{k})} \\ &\quad - i9\left(\frac{v\tilde{g}}{\Lambda}\right)^2\int \frac{d\omega}{2\pi}\frac{d^2\mathbf{k}}{(2\pi)^2}\Pi_g(\Omega,\mathbf{q}) \\ &\quad \times \frac{m_\sigma(\omega,\mathbf{k})}{\omega^2 - v^2\mathbf{k}^2 - m_\sigma^2(\omega,\mathbf{k})}. \end{aligned}$$

After Wick rotation, this equation is recast as

$$\begin{aligned} m_\sigma(\varepsilon,\mathbf{p}) &= \frac{4v\tilde{g}}{\Lambda}\int \frac{d\omega}{2\pi}\frac{d^2\mathbf{k}}{(2\pi)^2}\frac{m_\sigma(\omega,\mathbf{k})}{\omega^2 + v^2\mathbf{k}^2 + m_\sigma^2(\omega,\mathbf{k})} \\ &\quad - \frac{9}{4v^2}\left(\frac{v\tilde{g}}{\Lambda}\right)^2\int \frac{d\omega}{2\pi}\frac{d^2\mathbf{k}}{(2\pi)^2} \\ &\quad \times \frac{m_\sigma(\omega,\mathbf{k})\sqrt{v^2\mathbf{q}^2+\Omega^2}}{\omega^2 + v^2\mathbf{k}^2 + m_\sigma^2(\omega,\mathbf{k})}. \end{aligned} \tag{19}$$

The leading-order correction to dynamical gap generation has been previously analyzed in Ref. [53]. Notice there is a sign difference in the definition of $\tilde{g}$. In Ref. [53], a finite gap is generated only when $\tilde{g} < \tilde{g}_c = -\pi^2/4$ (in the limit of $N \to \infty$); in our case the critical value becomes $\tilde{g}_c = \pi^2/2$. In this work we only consider negative $\tilde{g}$, and thus the GN interaction cannot induce excitonic pairing by itself. However, the GN interaction might affect the fate of excitonic pairing induced by the Coulomb interaction. This will be studied in Sec. III A.

C. Yukawa coupling interaction near AFM QCP

When the strength of spinful GN interaction increases, the AFM correlation is enhanced. The gapless Dirac SM becomes an AFM Mott insulator once U exceeds some critical value U_c, which defines a zero-temperature AFM QCP. As revealed by Tang *et al.* [18], U_c appears to be an increasing function of α in the region of weak Coulomb interaction. Previous studies on such an AFM quantum criticality [12,54] demonstrated that the Yukawa coupling between the Dirac fermion and AFM quantum fluctuation, described by the scalar field ϕ, determines the low-energy properties of the AFM QCP if the Coulomb interaction is ignored. Here, we are particularly interested in whether the excitonic pairing is suppressed or promoted near the AFM QCP.

To describe the AFM fluctuation, we add to $\mathcal{L}_0$ the following Lagrangian density of ϕ field:

$$\mathcal{L}_b = -\phi\left(\partial_\tau^2 + v_\phi^2\nabla^2 + r\right)\phi - \frac{\lambda_0}{4!}\phi^4 + \sum_\sigma \lambda\phi\cdot\sigma\bar{\Psi}_\sigma\Psi_\sigma, \tag{20}$$

where λ is the strength parameter for Yukawa coupling interaction and $\sigma = \pm 1$ is fermion spin. The AFM order parameter [12,18] is given by $A = \langle\sum_\sigma \sigma\bar{\Psi}_\sigma\Psi_\sigma\rangle$. The scalar field ϕ stands for the quantum fluctuation around this mean value. The boson mass r can be identified as the tuning parameter for the SM-AFM transition, and $r = 0$ at the QCP. Here, we consider only the SM side of the QCP, and thus suppose $r \geqslant 0$. To facilitate analytical calculations, we introduce two new coupling constants for two spin components: $\lambda_\sigma = \lambda\sigma$. It is worth mentioning that λ_σ has the same dimension as $\sqrt{r}$.

Once $\mathcal{L}_b$ is introduced, the continual chiral symmetry is explicitly broken. Nevertheless, the total action still preserves a discrete chiral symmetry $\Psi_\sigma \to \gamma_5\Psi_\sigma$, as long as the scalar field ϕ transforms simultaneously in the following way: $\phi \to -\phi$. When a finite gap is generated via excitonic pairing, the above discrete chiral symmetry will be dynamically broken.

The Feynman diagrams of the fermion self-energy are shown in Fig. 4, where V stands for the dressed Coulomb interaction function and D_ϕ for the dressed propagator of the ϕ field. To the leading order of $1/N$ expansion, the dynamical gap satisfies the following DS equation:

$$m_\sigma(\varepsilon,\mathbf{p}) = \frac{i}{4}\int\frac{d\omega}{2\pi}\frac{d^2\mathbf{k}}{(2\pi)^2}\mathrm{Tr}[\gamma_0 G_\sigma(\omega,\mathbf{k})V(\Omega,\mathbf{q})\gamma_0] + \frac{i(\lambda_\sigma)^2}{4}\int\frac{d\omega}{2\pi}\frac{d^2\mathbf{k}}{(2\pi)^2}\mathrm{Tr}[G_\sigma(\omega,\mathbf{k})D_\phi(\Omega,\mathbf{q})], \tag{21}$$

where $\varepsilon = \Omega + \omega$ and $\mathbf{p} = \mathbf{q} + \mathbf{k}$.

The free propagator of the bosonic field ϕ is

$$D_\phi^0(\Omega,\mathbf{q}) = \frac{1}{\Omega^2 - v^2\mathbf{q}^2 - r^2}.$$

Similar to the long-range Coulomb interaction, here we assume the boson velocity equals the fermion velocity. This free propagator is also renormalized by the collective excitations. Including this effect leads to the following dressed bosonic propagator:

$$D_\phi(\Omega,\mathbf{q}) = \frac{1}{D_\phi^0(\Omega,\mathbf{q})^{-1} + \Pi_\phi(\Omega,\mathbf{q})}, \tag{22}$$

where the screening effect is embodied in the polarization function $\Pi_\phi(\Omega,\mathbf{q})$. To the leading order of $1/N$ expansion, the diagram of $\Pi_\phi(\Omega,\mathbf{q})$ is presented in Fig. 2, given by the integral

$$\Pi_\phi(\Omega,\mathbf{q}) = -\sum_\sigma\int\frac{d\omega}{2\pi}\frac{d^2\mathbf{k}}{(2\pi)^2}\mathrm{Tr}\big[\lambda_\sigma G_\sigma^0(\omega,\mathbf{k})\lambda_\sigma \times G_\sigma^0(\omega+\Omega,\mathbf{k}+\mathbf{q})\big]. \tag{23}$$

According to the detailed calculations presented in Appendix, Π_ϕ has the simple form

$$\Pi_\phi(\Omega,\mathbf{q}) = -\frac{N(\lambda_\sigma)^2}{v^2}\frac{\sqrt{v^2\mathbf{q}^2-\Omega^2}}{4}, \tag{24}$$

which is consistent with that obtained in Ref. [55].

After performing calculations, we get the gap equation

$$m_\sigma(\varepsilon,\mathbf{p}) = \int\frac{d\omega}{2\pi}\frac{d^2\mathbf{k}}{(2\pi)^2}\frac{m_\sigma(\omega,\mathbf{k})}{\omega^2+v^2\mathbf{k}^2+m_\sigma(\omega,\mathbf{k})^2} \times\frac{1}{\frac{|\mathbf{q}|}{2\pi v\alpha}+\frac{N}{8}\frac{\mathbf{q}^2}{\sqrt{\Omega^2+v^2\mathbf{q}^2}}} - (\lambda_\sigma)^2\int\frac{d\omega}{2\pi}\frac{d^2\mathbf{k}}{(2\pi)^2} \times\frac{m_\sigma(\omega,\mathbf{k})}{\omega^2+v^2\mathbf{k}^2+m_\sigma(\omega,\mathbf{k})^2} \times\frac{1}{\Omega^2+v^2\mathbf{q}^2+r^2+\frac{N(\lambda_\sigma)^2}{v^2}\frac{\sqrt{\Omega^2+v^2\mathbf{q}^2}}{4}}, \tag{25}$$

where Wick rotation has been performed. There is a minus sign in the contribution due to the Yukawa coupling interaction. Two important conclusions can be deduced. First, the Yukawa coupling tends to suppress excitonic pairing. Second, the Yukawa coupling by itself is not able to trigger excitonic pairing.

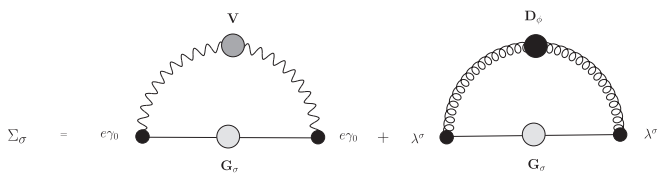

FIG. 4. Feynman diagram of the fermion self-energy due to Coulomb interaction and Yukawa coupling.

III. NUMERICAL RESULTS

In this section, we solve the DS equations numerically and analyze the physical implications of the solutions. We will first consider the case of weak GN interaction and then the vicinity of AFM QCP. Our aim is to determine their influence on the value of α_c. To make numerical evaluation easier, we carry out the following rescaling transformations:

$$\frac{m_\sigma}{v\Lambda} \to m_\sigma, \quad \frac{|\mathbf{p}|}{\Lambda} \to \mathbf{p}, \quad \frac{|\mathbf{k}|}{\Lambda} \to \mathbf{k}, \quad \frac{|\mathbf{q}|}{\Lambda} \to \mathbf{q},$$
$$\frac{\lambda_\sigma^2}{v\Lambda} \to \lambda_\sigma^2, \quad \frac{\omega}{v\Lambda} \to \omega, \quad \frac{\Omega}{v\Lambda} \to \Omega, \quad \frac{\varepsilon}{v\Lambda} \to \varepsilon. \tag{26}$$

By doing so, all the parameters that appear in the gap equations are made dimensionless.

A. Interplay of Coulomb and GN interactions

To examine the interplay between the long-range Coulomb and short-range GN interactions, we combine Eqs. (9) and (19), and then solve the total gap equation self-consistently for different values of $\tilde{g}$ at $N = 2$ and $\alpha = 2.2$, which are the physical flavor and the physical α of suspended graphene.

To simplify numerical evaluation, it is useful to first adopt the commonly used instantaneous approximation [22], which assumes that the fermion gap, the Coulomb interaction function, and the four-fermion interaction kernel are independent of energy. The impact of the energy dependence will be examined later. Under this approximation, the total gap equation can be written as

$$m_\sigma(\mathbf{p}) = \int \frac{d^2\mathbf{k}}{(2\pi)^2} \frac{m_\sigma(\mathbf{k})}{2\sqrt{\mathbf{k}^2 + m_\sigma(\mathbf{k})^2}} \frac{1}{\frac{|\mathbf{q}|}{2\pi\alpha} + \frac{N}{8}|\mathbf{q}|} + \tilde{g} \int \frac{d^2\mathbf{k}}{(2\pi)^2} \frac{m_\sigma(\mathbf{k})}{2\sqrt{\mathbf{k}^2 + m_\sigma^2(\mathbf{k})}} - \frac{9}{4}(\tilde{g})^2 \int \frac{d^2\mathbf{k}}{(2\pi)^2} \frac{|\mathbf{q}| m_\sigma(\mathbf{k})}{2\sqrt{\mathbf{k}^2 + m_\sigma^2(\mathbf{k})}}. \tag{27}$$

After solving this equation, we present the numerical results in Fig. 5, where m_0 is defined as the value of fermion gap at zero momentum. As $|\tilde{g}|$ grows, m_0 decreases considerably. This implies that weak GN interaction tends to suppress the excitonic gap. The α dependence of m_0 is shown in Fig. 6. We observe that, as GN interaction increases, the value of α_c will be slightly increased. When $\tilde{g} = -0.7$, we find that $\alpha_c = 2.0$.

The instantaneous approximation has been previously used in the DS study of excitonic gap generation [22]. Extensive works confirmed that the value of α_c obtained under this approximation is actually not far from that obtained by incorporating higher-order corrections. In this sense, the instantaneous approximation leads to a qualitatively reliable conclusion. Further, we have also solved the gap equation by incorporating the energy dependence of the gap function and the Coulomb interaction. The sub-leading-order correction due to spinful GN interaction exhibits a logarithmic dependence on the energy cutoff. Our numerical results show that increasing the energy cutoff more or less modifies the values of $\tilde{g}_c$ and α_c. However, the qualitative conclusion that GN interaction suppresses excitonic pairing is not changed. Here, we choose an energy cutoff $\Lambda_E = 10v\Lambda$.

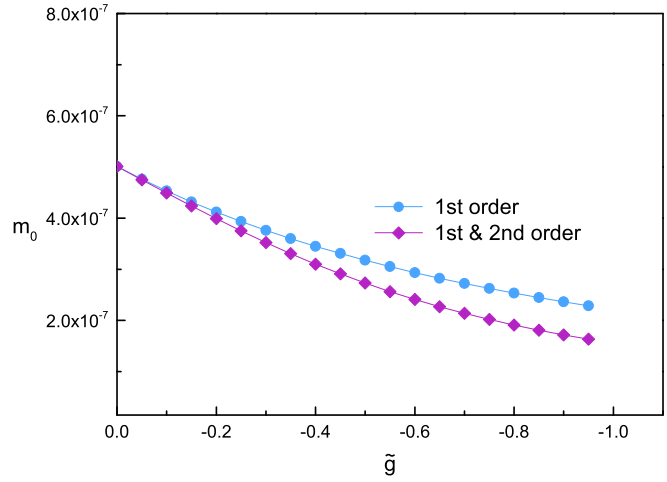

FIG. 5. The $\tilde{g}$ dependence of zero-momentum excitonic gap m_0 at $\alpha = 2.2$ and $N = 2$.

B. Interplay of Coulomb interaction and Yukawa coupling interaction near the AFM QCP

We now consider the interplay of Coulomb interaction and Yukawa coupling interaction. The corresponding DS gap equation is given by Eq. (25). Numerical calculations verify that the solution of this gap equation is insensitive to the energy cutoff. Below, the energy cutoff is taken as $\Lambda_E = 1000v\Lambda$.

To get a rapid glimpse of the main results, we will first neglect the energy dependence of both the fermion self-energy and the interaction functions. This approximation can be implemented by making the following

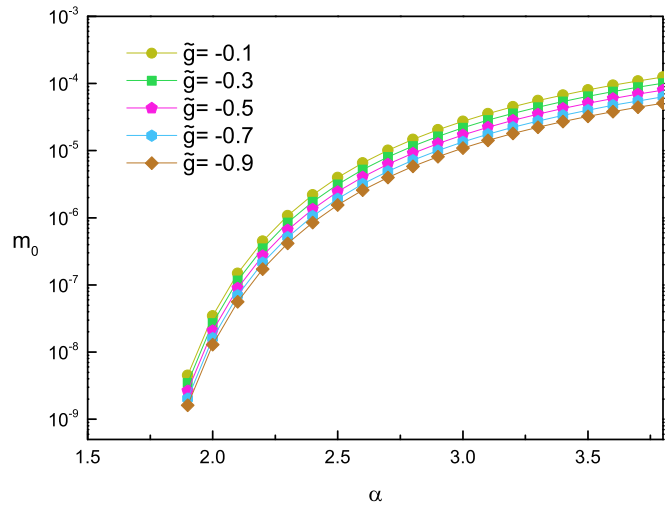

FIG. 6. The α dependence of zero-momentum gap m_0 for different values of $v\tilde{g}$ at $N = 2$.

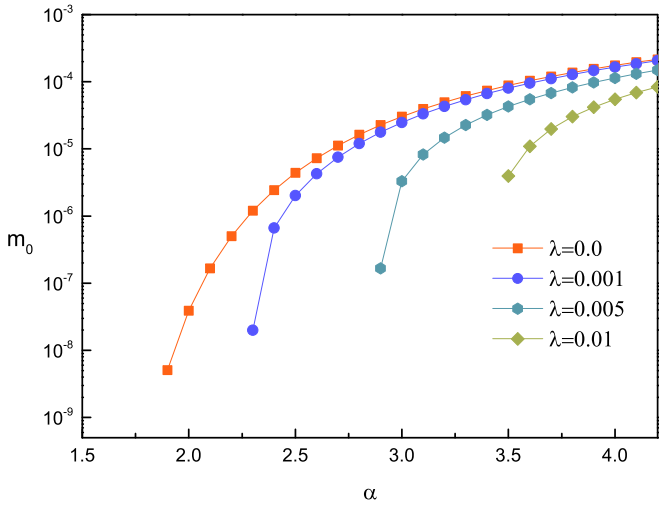

FIG. 7. The α dependence of m_0 for different values of λ at $N = 2$. Clearly, α_c is an increasing function of λ.

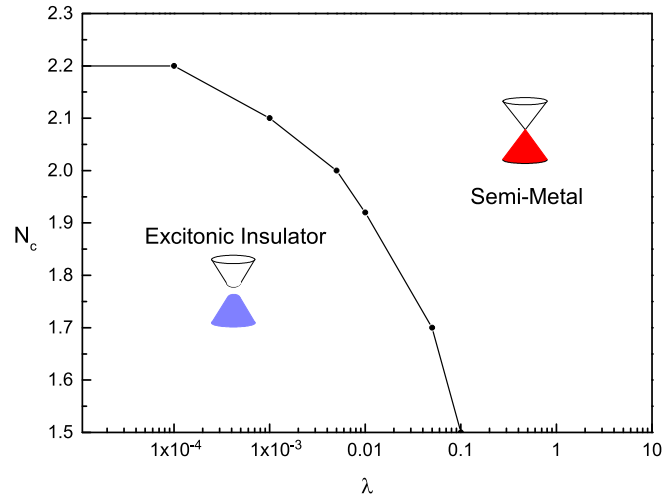

FIG. 8. The critical line of SM-EI transition on the λ-N plane. Here the Coulomb interaction parameter is fixed at $\alpha = 3.2$.

replacement:

$$m_\sigma(\varepsilon, \mathbf{p}) \to m_\sigma(\mathbf{p}), \tag{28}$$

$$V(\Omega, \mathbf{q}) \to V(\mathbf{q}), \tag{29}$$

$$D_\phi(\Omega, \mathbf{q}) \to D_\phi(\mathbf{q}). \tag{30}$$

Under this approximation, the DS gap equation becomes

$$\begin{aligned} m_\sigma(\mathbf{p}) = & \int \frac{d^2\mathbf{k}}{(2\pi)^2} \frac{m_\sigma(\mathbf{k})}{2\sqrt{\mathbf{k}^2 + m_\sigma(\mathbf{k})^2}} \frac{1}{\frac{|\mathbf{q}|}{2\pi\alpha} + \frac{N}{8}|\mathbf{q}|} \\ & - (\lambda_\sigma)^2 \int \frac{d^2\mathbf{k}}{(2\pi)^2} \frac{m_\sigma(\mathbf{k})}{2\sqrt{\mathbf{k}^2 + m_\sigma(\mathbf{k})^2}} \\ & \times \frac{1}{\mathbf{q}^2 + r^2 + N(\lambda_\sigma)^2 \frac{|\mathbf{q}|}{4}}. \end{aligned} \tag{31}$$

We have solved this equation numerically, and we show in Fig. 7 the α dependence of excitonic gap obtained at zero momenta, namely, $m(p = 0)$, for different values of λ. If the AFM QCP is entirely ignored, corresponding to $\lambda = 0$, the critical value $\alpha_c \approx 1.9$. If λ takes a very small value $\lambda = 0.001$, α_c is increased to $\alpha_c \approx 2.3$. For $\lambda = 0.005$ and 0.01, we find that $\alpha_c = 2.8$ and 3.5, respectively. Therefore, the excitonic gap generation can be significantly suppressed at the AFM QCP.

Further, we study how λ changes the critical fermion flavor N_c. We fix α at $\alpha = 3.2$, and solve Eq. (34) to obtain the relation between λ and N_c, with results presented in Fig. 8. For very small values of λ, $N_c \approx 2.2$. For $\lambda > 0.005$, N_c is reduced below 2. For Dirac fermions with physical flavor $N = 2$, the excitonic pairing cannot occur due to the presence of sufficiently strong Yukawa coupling interaction.

The dependence of α_c on λ at fixed flavor $N = 2$ is shown in Fig. 9. At the AFM QCP with $r = 0$, α_c increases rapidly as λ grows and finally goes to infinity at sufficiently large λ. This is another signature that AFM quantum criticality disfavors excitonic gap generation. As r increases, the system moves away from the AFM QCP into the SM region. In this process, the quantum fluctuation of the AFM order parameter is weakened, and the suppressing effect of excitonic pairing becomes progressively unimportant.

In Ref. [18], the authors found that the Coulomb interaction tends to increase U_c. Here our finding is that AFM quantum fluctuation suppresses excitonic pairing. There seems to be a repulsion between the excitonic pairing and the AFM ordering. Based on these results, we plot a schematic phase diagram on the U-α plane in Fig. 1. The critical line of U_c goes rightwards as α increases [18], whereas the critical line of α_c goes upwards as $U \to U_c$ from the left side. A previous RG study [12] predicted that the Dirac fermion system may undergo a first-order transition from EI to AFM Mott insulator. Our results indicate that such a direct transition does not occur and that the excitonic insulating phase and AFM Mott insulating phase are actually separated by an intermediate gapless SM phase.

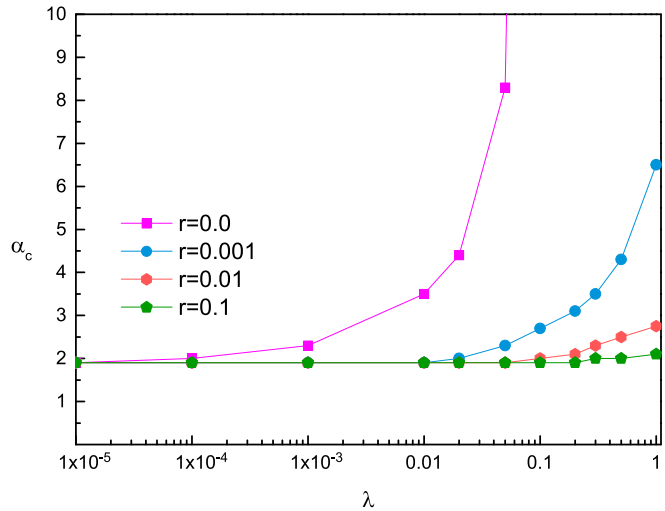

FIG. 9. The λ dependence of α_c at a number of values of r. Here the fermion flavor is $N = 2$.

We have also numerically solved Eq. (25), in which $\alpha_c = 0.7$ at $\lambda = 0$, and reached the same conclusion that the quantum AFM criticality tends to suppress excitonic gap generation. Therefore, the schematic phase diagram presented in Fig. 1 is still qualitatively correct after taking the energy dependence into account.

IV. APPLICATION OF THE RESULTS

Determination of the precise value of α_c proves to be a highly nontrivial challenge. In QED_3, the fermion propagator and the gauge boson propagator are coupled to each other by a set of DS integral equations [56]. The same is true for our case, since the Coulomb interaction can be effectively described by the coupling between the Dirac fermion and the temporal component of the U(1) gauge boson. The full fermion propagator has the following generic form:

$$G(\varepsilon, \mathbf{p}) = \frac{1}{\gamma_0 \varepsilon Z(\varepsilon, \mathbf{p}) - v(\gamma_1 p_x + \gamma_2 p_y) A(\varepsilon, \mathbf{p}) - m(\varepsilon, \mathbf{p})},$$

where $Z(\varepsilon, \mathbf{p})$ and $A(\varepsilon, \mathbf{p})$ are the wave-function renormalizations and $m(\varepsilon, \mathbf{p})$ is the fermion gap function. The dressed boson propagator is given by Eq. (6), where the polarization function should be replaced by the full one. The full polarization is determined by the dressed fermion propagator and the interaction vertex function Γ. Once the expression for vertex function is known, the dressed fermion and boson propagators could be determined. In practice, it is not possible to obtain the exact solutions of the coupled DS equations, and one always needs to introduce certain approximations (truncations) to replace the full propagators and the full vertex function with approximate ones. In the literature there are two commonly used vertex functions: the bare vertex and the Ball-Chiu [57] vertex.

Extensive DS equation studies of excitonic pairing in graphene have revealed that the precise value of α_c is very sensitive to the specific approximation. To demonstrate this, we list in Table I a number of representative values of α_c obtained by employing various approximations. If one assumes $Z = A = 1$ and ignores the vertex correction, the critical value $\alpha_c = 1.9$ in the instantaneous approximation and $\alpha_c = 0.7$ after including the energy dependence. Two of the authors [29] have incorporated Z and A, utilized the first term of Ball-Chiu vertex, and adopted the RPA expression of polarization Π_c. Under such approximations, it was found [29] that $\alpha \approx 3.2$. It was pointed out in Ref. [29] that α_c could be considerably decreased if the feedback of the excitonic gap on Π_c is included. Recently, Carrington *et al.* [33] have carried out more refined DS equation calculations after taking into account Z, A, the first term of the Ball-Chiu vertex, and also the feedback effects of Z, A, and m on Π_c, and obtained $\alpha_c \approx 2.06$. It is surprising that the value $\alpha_c = 1.9$ obtained in the present paper by employing the crude instantaneous approximation is actually quite close to the above result. Moreover, the value α_c obtained by Carrington *et al.* [33] is smaller than the physical value $\alpha = 2.16$ of suspended graphene. In the light of this result, one might have to conclude that clean, undoped suspended graphene is an EI at low temperatures.

TABLE I. DS equation results for the critical value α_c at the flavor $N = 2$. Z, A, m, and α are defined in the context. Γ_{BC} stands for the Ball-Chiu vertex correction. Π_c^{RPA} is the RPA-level polarization given by Eq. (8), and Π_c^{SC} represents the polarization function obtained from self-consistent DS equation calculations. The symbol $\otimes$ refers to the instantaneous approximation, and $\surd$ indicates that the energy dependence is taken into account. The corresponding function is neglected if the space is left blank.

Z	A	m	Γ_{BC}	Π_c^{SC}	Π_c^{RPA}	α	Reference
		$\otimes$			$\otimes$	1.9	Current paper
		$\otimes$			$\surd$	0.92	[35]
		$\surd$			$\surd$	0.7	Current paper
$\surd$	$\surd$	$\surd$	$\surd$		$\surd$	3.2	[29]
$\surd$	$\surd$	$\surd$	$\surd$		$\surd$	2.9	[32]
$\surd$	$\surd$	$\surd$	$\surd$	$\otimes$		1.99	[33]
$\surd$	$\surd$	$\surd$	$\surd$	$\surd$		2.06	[33]

Ellias *et al.* [21] has measured the cyclotron mass in suspended graphene and found no evidence of a finite gap at rather low energies ($\sim$0.1 meV). This finding was further supported by the measurements of Mayorov *et al.* [49]. How can one reconcile the recent theoretical result of Carrington *et al.* [33] and these experiments?

Here we propose that the seeming discrepancy can be explained by noticing the fact that graphene is not far from the AFM QCP. Wehling *et al.* [50] has calculated the on-site interaction parameter U in suspended graphene by using three different approaches. The critical value U_c needed to trigger AFM Mott transition seems to be only slightly larger than the physical U [18], which implies that realistic graphene is close to the AFM QCP [18]. Apparently, the AFM quantum fluctuation is important in graphene and should be seriously considered in the study of EI transition. As revealed in our calculations, AFM quantum fluctuation can strongly suppress excitonic pairing by increasing the value of α_c. Therefore, we conclude that the gapless SM state of suspended graphene is actually quite robust.

V. SUMMARY AND DISCUSSION

In summary, we have investigated the nonperturbative effect of dynamical excitonic gap generation in a 2D Dirac fermion system. The Dirac fermions are subjected to two types of interactions, namely, the long-range Coulomb interaction and the short-range on-site interaction. The former interaction can trigger excitonic pairing, whereas the latter leads to AFM Mott insulating quantum phase transition in the strong-coupling regime. The DS equation approach is employed to study the influence of on-site interaction on the fate of excitonic gap generation. We first have shown that the critical Coulomb interaction strength α_c is slightly suppressed by the weak GN interaction. As the system approaches the AFM QCP, the dynamics of Dirac fermions is strongly influenced by the quantum critical fluctuation of AFM order parameter. We have demonstrated that excitonic gap generation is suppressed by the AFM quantum fluctuation. Such a suppression effect is most significant at the AFM QCP but gradually diminishes when the system moves away from the QCP. If the 2D Dirac fermion system is close to the AFM QCP, as what happens in graphene, it would be very difficult to generate a finite excitonic gap.

Based on these results, we provide supplementary information to the global phase diagram reported in Ref. [18]. On the phase diagram, the EI phase is not neighboring to the AFM phase but is separated from the AFM phase by an intermediate gapless SM phase, as illustrated schematically in Fig. 1. This conclusion is different from the one previously stated in Ref. [12]. As indicated by our results, it is hardly possible to transform a 2D Dirac fermion system from an EI phase directly to an AFM Mott insulating phase. The reason is that the quantum critical AFM fluctuation can effectively prevent excitonic pairing.

When both α and U take large values, the Dirac fermion system could either be a AFM Mott insulator or a CDW. It might still be a gapless SM. To determine the quantitatively more precise phase diagram in such a strongly interacting regime, it is necessary to investigate the mutual influence between strong Coulomb interaction and strong on-site interaction in a more self-consistent manner, which will be carried out in future work.

ACKNOWLEDGMENTS

The numerical calculations were mainly performed on the supercomputing system of the Supercomputing Center of the University of Science and Technology of China. The authors acknowledge financial support from the National Natural Science Foundation of China under Grants No. 11847234, No. 11574285, and No. 11504379, and the Anhui Provincial Natural Science Foundation under Grant No. 1908085QA16.

APPENDIX: CALCULATION OF THE POLARIZATION Π_ϕ

We now provide the calculational details of the polarization function for the dressed propagator of bosonic AFM fluctuation. To the leading order of $1/N$ expansion, this polarization is defined as

$$\begin{aligned} i\Pi_\phi(\Omega,\mathbf{q}) &= -\sum_\sigma \int \frac{d\omega}{2\pi}\frac{d^2\mathbf{k}}{(2\pi)^2}\mathrm{Tr}\left[\lambda_\sigma G_\sigma^0(\omega,\mathbf{k})\lambda_\sigma G_\sigma^0(\omega+\Omega,\mathbf{k}+\mathbf{q})\right] \\ &= -\sum_\sigma \int \frac{d\omega}{2\pi}\frac{d^2\mathbf{k}}{(2\pi)^2}\mathrm{Tr}\left[\lambda_\sigma \frac{1}{-\gamma_0\omega+v\gamma\mathbf{k}+m_e}\lambda_\sigma \frac{1}{-\gamma_0(\omega+\Omega)+v\gamma(\mathbf{k}+\mathbf{q})+m_e}\right], \end{aligned} \tag{A1}$$

where m_e is a constant mass of Dirac fermion. Making the replacements $\mathbf{q}=v\mathbf{q}$ and $\mathbf{k}=v\mathbf{k}$, we rewrite it in the form

$$\begin{aligned} i\Pi_\phi(\Omega,\mathbf{q}) &= -\sum_\sigma \int \frac{d\omega}{2\pi}\frac{d^2\mathbf{k}}{(2\pi)^2}\mathrm{Tr}\left[\frac{\lambda_\sigma}{v^2}\frac{1}{-\gamma_0\omega+\gamma\mathbf{k}+m_e}\lambda_\sigma \frac{1}{-\gamma_0(\omega+\Omega)+\gamma(\mathbf{k}+\mathbf{q})+m_e}\right] \\ &= -4\sum_\sigma\left(\frac{\lambda_\sigma}{v}\right)^2 \int \frac{d\omega}{2\pi}\frac{d^2\mathbf{k}}{(2\pi)^2}\frac{\left((\Omega+\omega)\omega-(\mathbf{k}+\mathbf{q})\cdot\mathbf{k}+m_e^2\right)}{\left((\Omega+\omega)^2-(\mathbf{k}+\mathbf{q})^2-m_e^2\right)\left(\omega^2-\mathbf{k}^2-m_e^2\right)}. \end{aligned} \tag{A2}$$

Making use of the Feynman integral

$$\frac{1}{AB}=\int_0^1 dx\frac{1}{[(1-x)A+xB]^2}, \tag{A3}$$

we proceed as follows:

$$\begin{aligned} i\Pi_\phi &= -4\sum_\sigma\left(\frac{\lambda_\sigma}{v}\right)^2 \int_0^1 dx\int \frac{d\omega}{2\pi}\frac{d^2\mathbf{k}}{(2\pi)^2}\frac{\left[(\Omega+\omega)\omega-(\mathbf{k}+\mathbf{q})\cdot\mathbf{k}+m_e^2\right]}{\left[x(\Omega+\omega)^2-x(\mathbf{k}+\mathbf{q})^2-xm_e^2+(1-x)\omega^2-(1-x)\mathbf{k}^2-(1-x)m_e^2\right]^2} \\ &= -4\sum_\sigma\left(\frac{\lambda_\sigma}{v}\right)^2 \int_0^1 dx\int \frac{d\omega}{2\pi}\frac{d^2\mathbf{k}}{(2\pi)^2}\frac{\left[(\Omega+\omega)\omega-(\mathbf{k}+\mathbf{q})\cdot\mathbf{k}+m_e^2\right]^2}{\left[(x-x^2)(\Omega^2-\mathbf{q}^2)+(\omega+x\Omega)^2-(\mathbf{k}+x\mathbf{q})^2-m_e^2\right]^2}. \end{aligned} \tag{A4}$$

Defining $\omega'=\omega+x\Omega$ and $\mathbf{k}'=\mathbf{k}+x\mathbf{q}$, we further get

$$\begin{aligned} i\Pi_\phi &= -4\sum_\sigma\left(\frac{\lambda_\sigma}{v}\right)^2 \int_0^1 dx\int \frac{d\omega'}{2\pi}\frac{d^2\mathbf{k}'}{(2\pi)^2}\frac{(\omega'-x\Omega)[\omega'+(1-x)\Omega]-[\mathbf{k}'+(1-x)\mathbf{q}]\cdot(\mathbf{k}'-x\mathbf{q})+m_e^2}{\left((x-x^2)(\Omega^2-\mathbf{q}^2)+(\omega')^2-\mathbf{k}'^2-m_e^2\right)^2} \\ &= -4\sum_\sigma\left(\frac{\lambda_\sigma}{v}\right)^2 \int_0^1 dx\int \frac{d\omega'}{2\pi}\frac{d^2\mathbf{k}'}{(2\pi)^2}\frac{\omega'^2+(1-2x)\Omega\omega'-x(1-x)\Omega^2-\mathbf{k}'^2-(1-2x)\mathbf{q}\cdot\mathbf{k}'+x(1-x)\mathbf{q}^2+m_e^2}{\left[(x-x^2)(\Omega^2-\mathbf{q}^2)+\omega'^2-\mathbf{k}'^2-m_e^2\right]^2}. \end{aligned} \tag{A5}$$

Introducing $C=\sqrt{(x-x^2)(\Omega^2-\mathbf{q}^2)-\mathbf{k}'^2-m_e^2}$ leads to

$$i\Pi_\phi = 4\sum_\sigma\left(\frac{\lambda_\sigma}{v}\right)^2 \int_0^1 dx\int \frac{d\omega'}{2\pi}\frac{d^2\mathbf{k}'}{(2\pi)^2}\left[\frac{\omega'^2}{(\omega'^2+C^2)^2}-\frac{(x-x^2)(\Omega^2-\mathbf{q}^2)+\mathbf{k}'^2-m_e^2}{(\omega'^2+C^2)^2}\right].$$

Since

$$\int_{-\infty}^{+\infty} dx \frac{x^2}{(x^2+a^2)^2} = \frac{\pi}{2a}, \quad \int_{-\infty}^{+\infty} dx \frac{1}{(x^2+a^2)^2} = \frac{\pi}{2a^3}, \tag{A6}$$

we find that

$$\begin{aligned} i\Pi_\phi &= -4\sum_\sigma \left(\frac{\lambda_\sigma}{v}\right)^2 \int_0^1 dx \int \frac{d^2\mathbf{k}'}{(2\pi)^3}\left[\frac{\pi}{2C} - \frac{\pi(C^2+2\mathbf{k}'^2)}{2C^3}\right] \\ &= 4\sum_\sigma \left(\frac{\lambda_\sigma}{v}\right)^2 \int_0^1 dx \int \frac{d^2\mathbf{k}'}{(2\pi)^3} \frac{2\pi\mathbf{k}'^2}{2\sqrt{\left[(x-x^2)(\Omega^2-\mathbf{q}^2)-\mathbf{k}'^2-m_e^2\right]^3}}. \end{aligned}$$

After carrying out a series of calculations, we eventually obtain

$$i\Pi_\phi = -\frac{iN(\lambda_\sigma)^2}{8v^2}\left[\Lambda - 2\sqrt{\mathbf{q}^2-\Omega^2-m_e^2}\right], \tag{A7}$$

where Λ is the ultraviolet momentum cutoff. In the massless limit, i.e., $m_e = 0$, we have

$$\Pi_\phi = -\frac{N(\lambda_\sigma)^2}{4v^2}\sqrt{v^2\mathbf{q}^2-\Omega^2}. \tag{A8}$$

After Wick rotation ($\Omega \to i\Omega$), we can have the polarization function in Euclidean space,

$$\Pi_\phi^E = -\frac{N(\lambda_\sigma)^2}{4v^2}\sqrt{v^2\mathbf{q}^2+\Omega^2}. \tag{A9}$$

[1] P. A. Lee, N. Nagaosa, and X.-G. Wen, Rev. Mod. Phys. **78**, 17 (2006).
[2] J. Orenstein and A. J. Millis, Science **288**, 468 (2000).
[3] K. S. Novoselov, A. K. Geim, S. V. Morozov, D. Jiang, Y. Zhang, S. V. Dubonos, I. V. Grigorieva, and A. A. Firsov, Science **306**, 666 (2004).
[4] K. S. Novoselov, A. K. Geim, S. V. Morozov, D. Jiang, M. I. Katsnelson, I. V. Grigorieva, S. V. Dubonos, and A. A. Firsov, Nature (London) **438**, 197 (2005).
[5] A. H. Castro Neto, F. Guinea, N. M. R. Peres, K. S. Novoselov, and A. K. Geim, Rev. Mod. Phys. **81**, 109 (2009).
[6] S. Das Sarma, S. Adam, E. H. Hwang, and E. Rossi, Rev. Mod. Phys. **83**, 407 (2011).
[7] V. N. Kotov, B. Uchoa, V. M. Pereira, F. Guinea, and A. H. Castro Neto, Rev. Mod. Phys. **84**, 1067 (2012).
[8] M. Z. Hasan and C. L. Kane, Rev. Mod. Phys. **82**, 3045 (2010).
[9] M. Hirata, K. Ishikawa, K. Miyagawa, M. Tamura, C. Berthier, D. Basko, A. Kobayashi, G. Matsuno, and K. Kanoda, Nat. Commun. **7**, 12666 (2016).
[10] R. Shankar, Rev. Mod. Phys. **66**, 129 (1994).
[11] C. A. Downing and M. E. Portnoi, Phys. Status Solidi B 1800584 (2019), doi: 10.1002/pssb.201800584.
[12] I. F. Herbut, Phys. Rev. Lett. **97**, 146401 (2006).
[13] T. Sato, M. Hohenadler, and F. F. Assaad, Phys. Rev. Lett. **119**, 197203 (2017).
[14] S. Raghu, X.-L. Qi, C. Honerkamp, and S.-C. Zhang, Phys. Rev. Lett. **100**, 156401 (2008).
[15] C. Weeks and M. Franz, Phys. Rev. B **81**, 085105 (2010).
[16] A. G. Grushin, E. V. Castro, A. A. Cortijo, F. de Juan, M. A. H. Vozmediano, and B. Valenzuela, Phys. Rev. B **87**, 085136 (2013).
[17] M. Daghofer and M. Hohenadler, Phys. Rev. B **89**, 035103 (2014).
[18] H.-K. Tang, J. N. Leaw, J. N. B. Rodrigues, I. Herbut, P. Sengupta, F. F. Assaad, and S. Adam, Science **361**, 570 (2018).
[19] P. Buividovich, D. Smith, M. Ulybyshev, and L. von Smekal, Phys. Rev. B **98**, 235129 (2018).
[20] T.-S. Zeng, W. Zhu, and D. Sheng, npj Quant Mater **3**, 49 (2018).
[21] D. C. Elias, R. V. Gorbachev, A. S. Mayorov, S. V. Morozov, A. A. Zhukov, P. Blake, L. A. Ponomarenko, I. V. Grigorieva, K. S. Novoselov, F. Guinea, and A. K. Geim, Nat. Phys. **7**, 701 (2011).
[22] D. V. Khveshchenko, Phys. Rev. Lett. **87**, 246802 (2001).
[23] E. V. Gorbar, V. P. Gusynin, V. A. Miransky, and I. A. Shovkovy, Phys. Rev. B **66**, 045108 (2002).
[24] D. V. Khveshchenko and H. Leal, Nucl. Phys. B **687**, 323 (2004).
[25] G.-Z. Liu, W. Li, and G. Cheng, Phys. Rev. B **79**, 205429 (2009).
[26] D. V. Khveshchenko, J. Phys.: Condens. Matter **21**, 075303 (2009).
[27] O. V. Gamayun, E. V. Gorbar, and V. P. Gusynin, Phys. Rev. B **81**, 075429 (2010).
[28] J. Sabio, F. Sols, and F. Guinea, Phys. Rev. B **82**, 121413(R) (2010).
[29] J.-R. Wang and G.-Z. Liu, New J. Phys. **14**, 043036 (2012).
[30] C. Popovici, C. S. Fischer, and L. von Smekal, Phys. Rev. B **88**, 205429 (2013).
[31] J. Gonzalez, Phys. Rev. B **92**, 125115 (2015).
[32] M. E. Carrington, C. S. Fischer, L. von Smekal, and M. H. Thoma, Phys. Rev. B **94**, 125102 (2016).
[33] M. E. Carrington, C. S. Fischer, L. von Smekal, and M. H. Thoma, Phys. Rev. B **97**, 115411 (2018).
[34] H.-X. Xiao, J.-R. Wang, H.-T. Feng, P.-L. Yin, and H.-S. Zong, Phys. Rev. B **96**, 155114 (2017).

[35] O. V. Gamayun, E. V. Gorbar, and V. P. Gusynin, Phys. Rev. B **80**, 165429 (2009).
[36] J. E. Drut and T. A. Lähde, Phys. Rev. Lett. **102**, 026802 (2009).
[37] J. E. Drut and T. A. Lähde, Phys. Rev. B **79**, 165425 (2009).
[38] J. E. Drut and T. A. Lähde, Phys. Rev. B **79**, 241405(R) (2009).
[39] W. Armour, S. Hands, and C. Strouthos, Phys. Rev. B **81**, 125105 (2010).
[40] W. Armour, S. Hands, and C. Strouthos, Phys. Rev. B **84**, 075123 (2011).
[41] P. V. Buividovich and M. I. Polikarpov, Phys. Rev. B **86**, 245117 (2012).
[42] M. V. Ulybyshev, P. V. Buividovich, M. I. Katsnelson, and M. I. Polikarpov, Phys. Rev. Lett. **111**, 056801 (2013).
[43] D. Smith and L. von Smekal, Phys. Rev. B **89**, 195429 (2014).
[44] I. S. Tupitsyn and N. V. Prokof'ev, Phys. Rev. Lett. **118**, 026403 (2017).
[45] F. de Juan and H. A. Fertig, Solid State Commun. **152**, 1460 (2012).
[46] A. V. Kotikov and S. Teber, Phys. Rev. D **94**, 114010 (2016).
[47] L. L. Marnham and A. V. Shytov, Phys. Rev. B **92**, 085409 (2015).
[48] C. A. Downing and M. E. Portnoi, Nat. Commun. **8**, 897 (2017).
[49] A. S. Mayorov, D. C. Elias, I. S. Mukhin, S. V. Morozov, L. A. Ponomarenko, K. S. Novoselov, A. K. Geim, and R. V. Gorbachev, Nano. Lett. **12**, 4629 (2012).
[50] T. O. Wehling, E. Sasioglu, C. Friedrich, A. I. Lichtenstein, M. I. Katsnelson, and S. Blügel, Phys. Rev. Lett. **106**, 236805 (2011).
[51] J. A. Gracey, Phys. Rev. D **97**, 105009 (2018).
[52] N. Dorey and R. D. Kenway, Nucl. Phys. B **333**, 419 (1990).
[53] K. Kaveh and I. F. Herbut, Phys. Rev. B **71**, 184519 (2005).
[54] I. F. Herbut, V. Juričić, and O. Vafek, Phys. Rev. B **80**, 075432 (2009).
[55] L. Fritz, Phys. Rev. B **83**, 035125 (2011)
[56] C. D. Roberts and A. G. Williams, Prog. Part. Nucl. Phys. **33**, 477 (1994).
[57] J. S. Ball and T. W. Chiu, Phys. Rev. D **22**, 2542 (1980).